

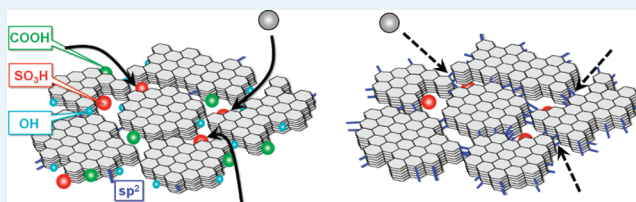
# Amorphous Carbon with SO<sub>3</sub>H Groups as a Solid Brønsted Acid Catalyst

Kiyotaka Nakajima and Michikazu Hara\*

Materials and Structures Laboratory, Tokyo Institute of Technology, Nagatsuta 4259-R3-33, Midori-ku, Yokohama 226-8503, Japan

**ABSTRACT:** Homogeneous Brønsted acid catalysts such as H<sub>2</sub>SO<sub>4</sub> and HCl are used for the production of industrially important chemicals. However, their use requires significant energy costs for separation, reuse, and treatment of salt wastes. Alternatively, heterogeneous Brønsted acid catalysts are promising candidates that can decrease the environmental impact associated with chemical production. In this review, we highlight amorphous carbon bearing SO<sub>3</sub>H groups as an insoluble Brønsted acid available for various acid-catalyzed reactions.

**KEYWORDS:** Brønsted acid, heterogeneous catalyst, sulfonic acid groups, amorphous carbon



## 1. INTRODUCTION

Homogeneous Brønsted acids such as H<sub>2</sub>SO<sub>4</sub> and HF are essential catalysts for the production of fuels and industrially important chemicals. However, the use of these catalysts requires energy-inefficient processes for separation, recycling, and treatment of the spent acids. Neutralization of the homogeneous acids produces sulfate wastes, and thus, the acids do not fulfill the general requirement of a catalyst as a reusable material that can repeatedly accelerate a chemical reaction. By this method, more than 15 million tons of H<sub>2</sub>SO<sub>4</sub>, for example, are consumed as an unrecyclable catalyst each year. A “green” approach to chemical processes has stimulated the use of recyclable strong solid acids as replacements for such unrecyclable “liquid acid” catalysts.<sup>1–8</sup> However, a major obstacle to such progress is the lack of a solid acid that is as active, stable, and inexpensive as sulfuric acid.

An ideal solid material for the applications considered here should have high stability and many strong protonic acid sites. Water is employed in many industrially important acid-catalyzed reactions, thus it is essential for the solid acid to maintain strong acidity, even in water. While organic acid/inorganic solid oxide hybrids and strong acidic cation-exchangeable resins including perfluorosulfonated ionomers (i.e., Nafion) have been studied extensively as promising approaches to the construction of desired solid acids or proton conductors,<sup>9–12</sup> such materials are expensive and the acid activities are still much lower than that of sulfuric acid,<sup>7</sup> and as such their practical utility has been limited. In this paper, we report the synthesis and performance of a carbon material with a high density of sulfonic acid groups (SO<sub>3</sub>H) as a novel, strong, and stable solid acid. A new strategy is adopted for the development of new types of solid acids: amorphous carbon materials consisting of small polycyclic aromatic carbon sheets with attached SO<sub>3</sub>H groups. This approach is simple and allows for the use of sulfoaromatic hydrocarbons—strong, stable solvent-soluble acids (e.g., benzene sulfonic acid and

naphthalene sulfonic acid)—as insoluble solid acids. The amorphous carbon materials based on such a new concept exhibit remarkable catalytic performance for various acid-catalyzed reactions, such as the esterification of higher fatty acids,<sup>13</sup> hydration,<sup>14</sup> and hydrolysis.<sup>15,16</sup> The particulate amorphous carbon with SO<sub>3</sub>H groups can be readily separated from reaction solutions by simple decantation or filtration, allowing repeated reuse of the material as a catalyst.

## 2. PREPARATION OF SO<sub>3</sub>H-BEARING AMORPHOUS CARBON

There are two routes for the preparation of amorphous carbon with SO<sub>3</sub>H groups; incomplete carbonization of sulfoaromatic compounds<sup>15</sup> and sulfonation of incompletely carbonized organic matter.<sup>13,14,16–42</sup> While the former can be used to prepare carbon material with a high density of SO<sub>3</sub>H groups (>4 mmol g<sup>-1</sup>), many problems still remain in large scale production and safety, because sulfoaromatic compounds are carbonized in concentrated H<sub>2</sub>SO<sub>4</sub> above 473 K. The latter route facilitates the preparation of SO<sub>3</sub>H-bearing amorphous carbon, although the amounts of acid are smaller than that of the former route (<2.5 mmol g<sup>-1</sup>).<sup>13</sup> Most of the amorphous carbon with SO<sub>3</sub>H groups reported is therefore prepared by sulfonation of incompletely carbonized organic matter. In this preparation, sugars,<sup>13,14,17,24,26,28,31,33,35,36,38–40,42</sup> starch,<sup>22,23,30</sup> cellulosic materials,<sup>16,18</sup> and polymers—anything that can be carbonized—can be used as starting materials.<sup>25,27,29,31,32,34</sup> Carbonization temperature dominates the catalytic performance of the material prepared by this method. Low carbonization temperatures (<ca. 523 K) only provide complex polymers containing aromatic compounds. Sulfonation of such pyrolysates results in soluble sulfonated species. In contrast,

Received: February 10, 2012

Revised: March 16, 2012

Published: April 18, 2012

high carbonization temperatures (>ca. 723 K) largely decrease the catalytic performance due to growth of the carbon network, as discussed later. Sulfonation of carbon materials with electrical conductivity, such as graphite, cannot form carbon sheets that bond high densities of  $\text{SO}_3\text{H}$  groups,<sup>15</sup> because carbon sheets with conducting electrons lose aromaticity.

### 3. STRUCTURE OF CELLULOSE-DERIVED CARBON SOLID ACID (CCSA)

Amorphous carbon bearing  $\text{SO}_3\text{H}$  groups can incorporate large amounts of hydrophilic molecules, including water, into the carbon bulk, due to the high densities of hydrophilic functional groups bonded to the flexible carbon sheets. Such incorporation provides good access by reactants in solution to the  $\text{SO}_3\text{H}$  groups, which gives rise to high catalytic performance for industrially important reactions, despite the small surface area of the material ( $<2 \text{ m}^2 \text{ g}^{-1}$ ).<sup>13,14,16</sup> The catalytic activity of the material is largely dependent on the carbonization temperature of the starting organic materials.<sup>14</sup> Here, we describe the correlation of the  $\text{SO}_3\text{H}$ -bearing amorphous carbon structure with the carbonization temperature before sulfonation. There are many reports on materials prepared from various starting materials; however, there is no significant structural dependence on the carbonization temperature among carbon materials with  $\text{SO}_3\text{H}$  groups. Figures 1A and B show X-ray diffraction

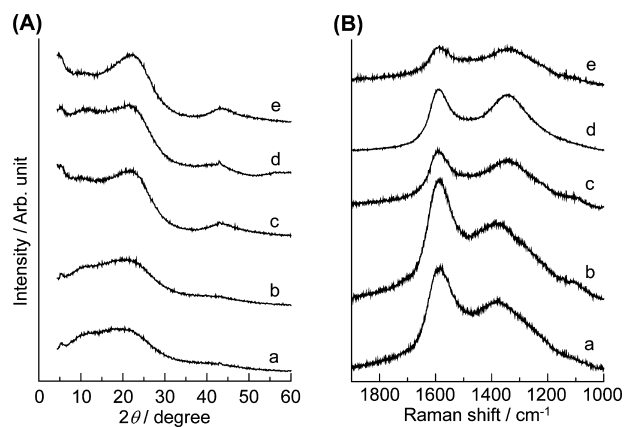


**Figure 1.** (A) XRD patterns and (B) Raman spectra for carbon solid acids prepared at different carbonization temperatures: (a) CCSA-673, (b) CCSA-723, (c) CCSA-823, (d) CCSA-873, and (e) CCSA-923.

(XRD) patterns and Raman spectra of cellulose-derived carbon solid acid (CCSA) samples. CCSA was prepared by partial carbonization of a microcrystalline cellulose powder (Avicel, Merck) and sulfonation of the resulting carbon precursor in fuming  $\text{H}_2\text{SO}_4$  solution. The microcrystalline cellulose was heated at 673–923 K for 5 h under flowing  $\text{N}_2$  to produce incompletely carbonized materials as precursors. The carbon precursors were then warmed in fuming  $\text{H}_2\text{SO}_4$  solution (15 wt %) at 353 K for 10 h.<sup>21</sup> In reality, sulfonation does not require such long time at the temperature because the introduced amounts of  $\text{SO}_3\text{H}$  groups reach a plateau. The resulting materials were washed repeatedly with hot distilled water until the pH of the filtrate became neutral, after which the filtrate was dried at 333 K for 12 h. CCSA samples were prepared at different carbonization temperatures of 673, 723, 823, 873, and 923 K, which are denoted as CCSA-673, -723, -823, -873, and -923, respectively. All the patterns have two broad and weak diffraction peaks at around  $20^\circ$  and  $45^\circ$ , which are assigned to

the graphitic (002) and (101) planes, respectively. Such diffraction patterns are typical of amorphous carbon consisting of disordered polycyclic aromatic carbon sheets.<sup>43</sup> The (002) and (101) diffraction peaks become clear with increasing carbonization temperature, due to stacking of carbon sheets. The Raman spectra of the samples have two distinct signals assignable to the D ( $1350 \text{ cm}^{-1}$ ,  $A_{1g}$  D breathing mode) and G ( $1580 \text{ cm}^{-1}$ ,  $E_{2g}$  G mode) bands, which indicate the presence of polycyclic aromatic carbon sheets in the carbon bulk.<sup>44</sup> Table 1

**Table 1.** Structural Parameters of Carbon Solid Acids Prepared at Different Carbonization Temperatures

	H/C ratio <sup>a</sup> /mmol $\text{g}^{-1}$	$\text{SO}_3\text{H}$ density <sup>b</sup> /mmol $\text{g}^{-1}$	$S_{\text{BET}}/\text{m}^2 \text{ g}^{-1}$	$L_a^c/\text{nm}$
CCSA-673	0.96	1.8	<5	1.2
CCSA-723	0.82	1.6	<5	1.2
CCSA-823	0.32	0.89	<5	1.3
CCSA-873	0.32	0.75	<5	1.3
CCSA-923	0.27	0.92	<5	1.3

<sup>a</sup>H/C ratio estimated by CHNS elemental analysis. <sup>b</sup>Sulfur content estimated by CHNS elemental analysis. <sup>c</sup>Average size of polycyclic aromatic carbon sheets in the CCSA sample.<sup>26</sup>

summarizes the structural parameters of the samples. These samples have small BET surface areas of less than  $5 \text{ m}^2 \text{ g}^{-1}$ ; all the samples exhibit a typical type II isotherm of nonporous materials, and the amount of  $\text{N}_2$  adsorbed at  $P/P_0 = 0.95\text{--}0.99$  is estimated to be ca.  $0.5 \text{ mL g}^{-1}$ . The samples are therefore regarded as bulk carbon materials that do not have micro, meso, and macroporous structures within the carbon bulk. The average size of the carbon sheets in the samples was estimated to be ca. 1.2–1.5 nm from the intensity ratio of the D and G bands,<sup>44</sup> which indicates that the carbon sheet size is not significantly dependent on the carbonization temperature in the range of 673–923 K. In contrast, the H/C ratio of the CCSA samples drops at the border between 723 and 823 K, which implies that an increase in the carbonization temperature does not result in an increase of the carbon sheet size, but does result in cross-linking between the carbon sheets under the experimental conditions.

Figure 2 shows  $^{13}\text{C}$  cross-polarization/magic angle spinning (CP/MAS) nuclear magnetic resonance (NMR) spectra for the samples. An intense broad signal at 130 ppm, assignable to polycyclic aromatic carbon, is evident in all spectra. In addition, the absence of signals for  $\text{sp}^3$ -derived carbons at 0–40 ppm indicates that most of the  $\text{sp}^3$ -carbons in cellulose are converted into aromatic  $\text{sp}^2$ -carbons during the carbonization treatment and cross-linking among the carbon sheets is due to  $\text{sp}^2$ -carbons. Two broad signals at 150 and 180 ppm, due to phenolic OH and COOH groups, are observed only in the spectra of CCSA-673 and -723 (Figures 2a and b); there are no phenolic OH and COOH groups in the samples prepared at >823 K. Figure 3A shows Fourier transform-infrared (FT-IR) absorption spectra for the dehydrated CCSA samples. The spectra for CCSA-673 and -723 (Figures 3Aa and b) have vibration bands at  $1167$  and  $1042 \text{ cm}^{-1}$ , which are identified as  $\text{O}=\text{S}=\text{O}$  symmetric stretching and  $\text{SO}_3^-$  stretching modes in  $\text{SO}_3\text{H}$ , respectively.<sup>16</sup> Although these peaks are also observed in other spectra (Figures 3Ac–g), they have weak intensities, due

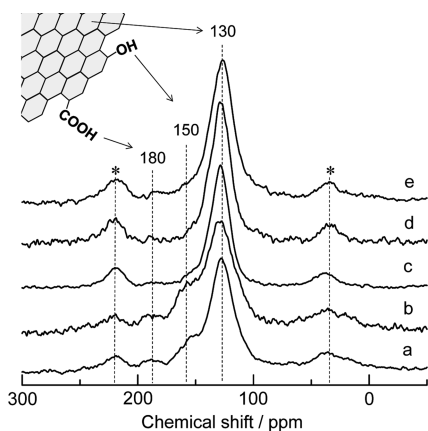


**Figure 2.**  $^{13}\text{C}$  CP/MAS NMR spectra for carbon solid acids prepared at different carbonization temperatures: (a) CCSA-673, (b) CCSA-723, (c) CCSA-823, (d) CCSA-873, and (e) CCSA-923. An asterisk denotes a spinning sideband.

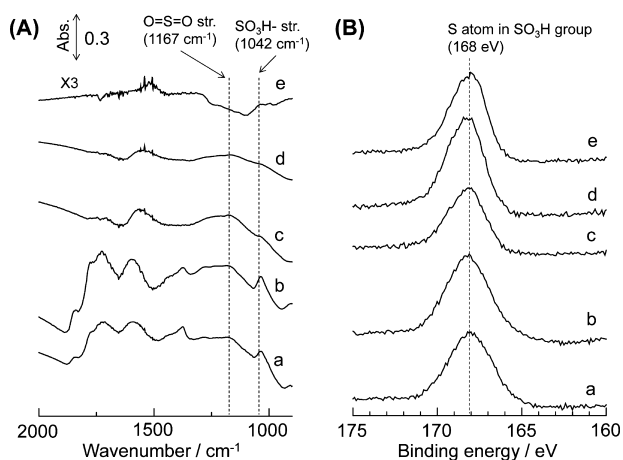


**Figure 3.** (A) FT-IR spectra and (B) XPS S 2p spectra for carbon solid acids prepared at different carbonization temperatures: (a) CCSA-673, (b) CCSA-723, (c) CCSA-823, (d) CCSA-873, and (e) CCSA-923.

to the efficient IR adsorption ability of the carbon frameworks formed by the high temperature treatment. X-ray photoelectron spectroscopy (XPS) spectra of the samples reveal a single S 2p peak at 168 eV (Figure 3B), which is attributable to sulfur in the  $\text{SO}_3\text{H}$  groups.<sup>14</sup> The amount of  $\text{SO}_3\text{H}$  groups in the CCSA samples is presented in Table 2; that for CCSA-673 and -723 is approximately twice that for CCSA-823 to -923.

It has been reported that CCSA can incorporate large amounts of hydrophilic molecules, including  $\text{H}_2\text{O}$ , as well as ion-exchangeable resins, due to a large amount of hydrophilic functional groups such as  $\text{SO}_3\text{H}$ , phenolic OH, and COOH groups.<sup>14,16,45</sup> To evaluate the incorporation capability of the prepared CCSA samples,  $\text{H}_2\text{O}$  adsorption was examined by adsorption–desorption isotherm experiments at 298 K, as shown in Figure 4. The isotherms of CCSA-673 and -723 in Figure 4A have typical type-II patterns, which are evident of nonporous solids; large amounts of  $\text{H}_2\text{O}$  are adsorbed even at low relative pressure and the amount of adsorbed  $\text{H}_2\text{O}$  increases in proportion to the relative pressure. This indicates that CCSA-673 and -723 have a strong affinity for water. The surface of graphite is generally hydrophobic,<sup>46</sup> and therefore, the  $\text{H}_2\text{O}$  vapor adsorption–desorption isotherm of pure graphitic carbon at 328 K has a well-defined type-III character,

**Table 2.** Catalytic Activities of CCSA Samples for the Esterification of Acetic Acid with Ethanol and the Hydrolysis of Cellobiose

	$\text{SO}_3\text{H}$ density <sup>a</sup> / $\text{mmol g}^{-1}$	esterification of acetic acid		hydrolysis of cellobiose	
		rate/ $\text{mmol min}^{-1} \text{g}^{-1}$	TOF/ $\text{min}^{-1}$	glucose yield <sup>b</sup> %	TOF <sup>c</sup> / $\text{min}^{-1}$
CCSA-673	1.8	1.79	1.0	35	0.092
CCSA-723	1.6	1.71	1.0	24	0.080
CCSA-823	0.89	0.046	0.074	6.7	0.029
CCSA-873	0.75	0.064	0.063	7.1	0.049
CCSA-923	0.92	0.062	0.058	2.4	0.020

<sup>a</sup>Sulfur content estimated by CHNS elemental analysis. <sup>b</sup>Glucose yield at 6 h. <sup>c</sup>TOF was estimated on the basis of the formation rate of glucose calculated by glucose yield.

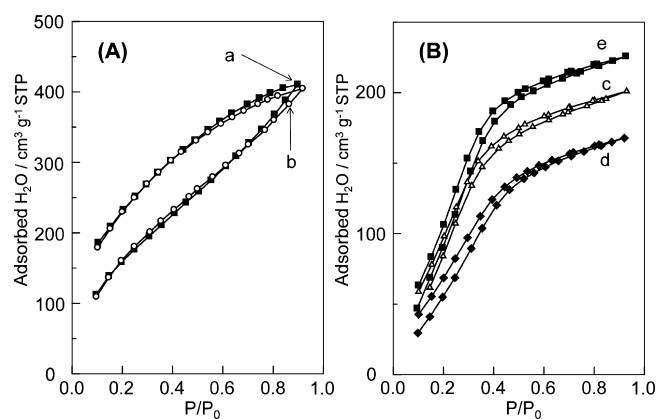


**Figure 4.**  $\text{H}_2\text{O}$  vapor adsorption–desorption isotherms for carbon solid acids prepared at different carbonization temperatures: (a) CCSA-673, (b) CCSA-723, (c) CCSA-823, (d) CCSA-873, and (e) CCSA-923.

where the amount of adsorbed  $\text{H}_2\text{O}$  is small at low  $P/P_0$  ( $<0.2$ ) and increases steeply at  $P/P_0 = 0.5–0.6$ .<sup>47</sup> Therefore, the strong affinity of CCSA-673 and -723 for  $\text{H}_2\text{O}$  is clearly derived from the large amounts of hydrophilic functional groups. The hysteresis loop in the CCSA-673 and -723 isotherms also supports the strong affinity for water. The strong interaction between physisorbed  $\text{H}_2\text{O}$  molecules and the hydrophilic functional groups indicates that  $\text{H}_2\text{O}$  adsorbed on the surface desorbs at lower  $P/P_0$  than that of adsorption. Assuming that the adsorption cross-sectional area of the  $\text{H}_2\text{O}$  molecule is  $0.125 \text{ nm}^2$ , then the surface areas of CCSA-673 and -723 at  $P/P_0 = 0.2$  are estimated to be 280 and  $260 \text{ m}^2 \text{ g}^{-1}$ , respectively, which are much larger than the BET surface areas determined from the  $\text{N}_2$  adsorption isotherms. While the isotherms of CCSA-823, -873, and -923 in Figure 4B also exhibit type-II patterns, these samples adsorb much smaller amounts of  $\text{H}_2\text{O}$  than CCSA-673 and -723 at low  $P/P_0$ , which suggests that these samples have lesser affinity for water than CCSA-673 and -723. However, these samples do adsorb large amounts of  $\text{H}_2\text{O}$  at high  $P/P_0$ , as do the CCSA-673 and -723 samples. This is due to the large capability for incorporation of hydrophilic molecules including  $\text{H}_2\text{O}$ ; therefore, these samples are also identified as nonporous carbon materials with large surface

areas under hydrophilic vapor atmosphere and in hydrophilic solution. The adsorption capacities of CCSA-673 and -723 are much larger than those of CCSA-823, -873, and -923, and this is probably due to the flexibility of the carbon framework. Despite their large adsorption capability for H<sub>2</sub>O vapor, all the samples do not have distinct micro, meso, and macroporous structures in the bulk under hydrophilic vapor atmosphere, because the adsorbed H<sub>2</sub>O is continuously increased in proportion to the relative pressure.

These results indicate that the sulfonation of cellulose carbonized at  $\leq 723$  K results in amorphous carbon composed of small carbon sheets (an average size between 1.2 and 1.3 nm) with phenolic OH, COOH groups in addition to SO<sub>3</sub>H groups. If the carbon material formed at 673 K is composed of uniformly functionalized carbon sheets, each graphene sheet is expected to bind three SO<sub>3</sub>H (1.8 mmol g<sup>-1</sup>) groups, three OH (2.0 mmol g<sup>-1</sup>) groups, and one COOH (0.4 mmol g<sup>-1</sup>) group. This is distinct from conventional solid acids with a single functional group. <sup>13</sup>C CP/MAS NMR results reveal that the carbon sheets are not linked by sp<sup>3</sup>-carbons, but sp<sup>2</sup>-carbons, as shown in Figure 5A. Sulfonation of the carbon precursors

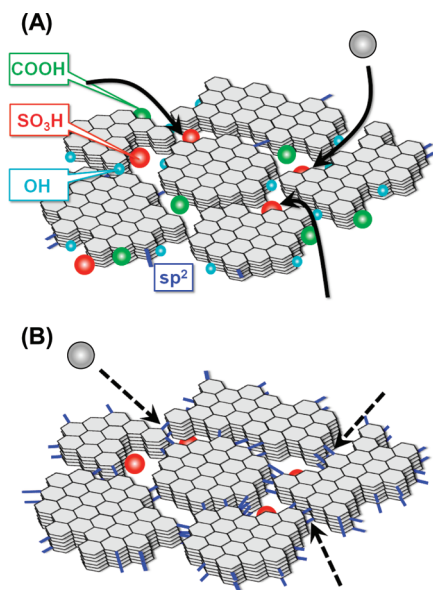


**Figure 5.** Schematic structures of proposed SO<sub>3</sub>H-bearing CCSA materials carbonized at different temperatures: (A) CCSA carbonized below 723 K and (B) CCSA carbonized above 823 K.

obtained at  $\geq 823$  K also forms amorphous carbon consisting of small carbon sheets, the size of which is the same as those obtained at  $\leq 723$  K. However, these carbon sheets have no phenolic OH and COOH groups, which results in increased sp<sup>2</sup> cross-linking among the carbon sheets, and the amount of SO<sub>3</sub>H groups bonded to the sheets is approximately half that of the samples carbonized at  $\leq 723$  K (Figure 5B).

Thus, although the carbon material prepared below 723 K is similar to that obtained above 823 K, there are distinct differences in the characteristics of both materials. Figure 6 shows <sup>1</sup>H MAS NMR spectra of the CCSA samples exposed to a water saturated atmosphere at room temperature for 2 days. The spectra for CCSA-673 and -723 have an intense signal at 6.8 ppm assignable to H<sub>3</sub>O<sup>+</sup>.<sup>48,49</sup> However, the corresponding signal is not observed for the CCSA-823, -873, and -923 samples, which indicates that adsorbed H<sub>2</sub>O cannot access the

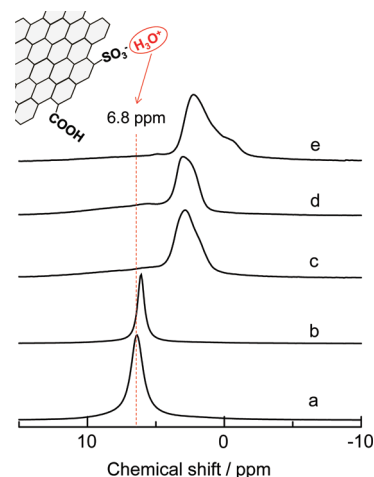


**Figure 6.** <sup>1</sup>H MAS NMR spectra for H<sub>2</sub>O-adsorbed CCSA samples: (a) CCSA-673, (b) CCSA-723, (c) CCSA-823, (d) CCSA-873, and (e) CCSA-923.

SO<sub>3</sub>H groups; the signal for adsorbed H<sub>2</sub>O is up-shifted with increasing carbonization temperature. Negative chemical shift for <sup>1</sup>H resonances have been observed on other carbonaceous materials, such as water on cokes and a variety of molecules adsorbed on the basal plane of graphitic carbon black,<sup>50–52</sup> where the adsorbed molecules are influenced by the strongly diamagnetic properties of the graphite structure.<sup>53</sup> Similarly, H<sub>2</sub>O introduced to CCSA-823, -873, and -923 cannot be directly adsorbed on the Brønsted acid sites but is adsorbed on the amorphous carbon, despite the presence of SO<sub>3</sub>H groups. This means that the SO<sub>3</sub>H groups in these materials cannot attack hydrophilic molecules, including water, even though there is a sufficient amount of SO<sub>3</sub>H groups.

#### 4. CORRELATION OF CATALYTIC PERFORMANCE WITH STRUCTURE

The catalytic performance of the CCSA samples was examined with respect to the esterification of acetic acid with ethanol (353 K) and the hydrolysis of cellobiose (373 K). Cellobiose is a water-soluble β-1,4 glucan where two glucose molecules are linked by β-1,4 glycosidic bonds, as with cellulose, a water-insoluble long β-1,4 glucan. While many cellulases effectively hydrolyze cellulose into shorter β-1,4 glucan, they are not so effective for the production of concentrated glucose solution by the hydrolysis of cellobiose for biological reasons. The symmetry of cellobiose due to the β-1,4 glycosidic bonds makes the hydrolysis of cellobiose more difficult than that of maltose, an asymmetrical glucose dimer with α-1,4 glycosidic bonds. For the same reason, the hydrolysis of cellulose is more difficult than that of starch, a glucose polymer with α-1,4 glycosidic bonds.

Table 2 lists the catalytic activities and amount of SO<sub>3</sub>H groups for the CCSA samples. According to the catalytic performance, the CCSA samples were clearly classified into two groups; CCSA-673 and -723; CCSA-823, -873, and -923. This distinct activity is also observed for glucose-derived amorphous carbon with SO<sub>3</sub>H groups,<sup>14</sup> although it is not yet clear whether this tendency is based on the carbonization temperature. The former group exhibited higher catalytic activities for both reactions, whereas those of the latter group were much lower, although they have sufficient amounts of SO<sub>3</sub>H groups. The amounts of SO<sub>3</sub>H groups in the latter CCSA group was

approximately half that of the former CCSA group, and the turnover frequency (TOF) for esterification was at least 10% lower than that of the former CCSA group. The same tendency was observed for the hydrolysis reaction. The  $\text{SO}_3\text{H}$  groups in CCSA-673 and -723 exhibit much higher reactivity than those in CCSA-823, -873, and -923. These results indicate that most of the  $\text{SO}_3\text{H}$  groups in the CCSA catalysts obtained by carbonization at  $\geq 823$  K are bonded to the carbon sheets and are not located where incorporated or adsorbed molecules can easily access, which results in poor catalytic performance. This is observed in all the acid-catalyzed reactions using amorphous carbon with  $\text{SO}_3\text{H}$ ; carbon catalysts prepared at ca. 673–723 K exhibit the highest catalytic activities.<sup>14–19,21,24,26,28,29,33,36–42</sup>

One possible explanation for this phenomenon is an increase in cross-linking between the carbon sheets above ca. 823 K. CCSA-823, -873, and -923 have highly cross-linked polycyclic aromatic carbon structures, which would prevent incorporation of reactants into the carbon bulk and access of the reactants to  $\text{SO}_3\text{H}$  groups. This also suggests that the  $\text{SO}_3\text{H}$  groups in these carbon materials are surrounded by densely cross-linked polycyclic aromatic carbon sheets. While there is no significant difference in  $\text{SO}_3\text{H}$  density among CCSA-823, -873, and -923, CCSA-923 is inferior to CCSA-873 in catalytic activity. Judging from H/C ratio in Table 1 (CCSA-873: H/C = 0.32. CCSA-923: H/C = 0.27), CCSA-923 is expected to have more cross-linked carbon network than CCSA-873: increase in cross-linking decreases the reactivity of  $\text{SO}_3\text{H}$  groups. A large amount of  $\text{H}_2\text{SO}_4$  can be intercalated into the interlayers between large carbon sheets in well-crystallized graphite through the formation of cationic carbon sheet– $\text{HSO}_4^-$ – $\text{H}_2\text{SO}_4$  complexes;<sup>54</sup> therefore, highly cross-linked polycyclic aromatic carbon sheets could also be sulfonated with  $\text{H}_2\text{SO}_4$ . However, neutral organic reactant molecules cannot access the  $\text{SO}_3\text{H}$  groups in this type of carbon bulk. Therefore, the aggregation of small carbon sheets with poor cross-linking would provide greater promise for carbon solid acids as highly active catalysts.

## 5. CATALYSIS WITH CCSA

**5.1. Hydrolysis of  $\beta$ -1,4 Glucan.** Amorphous carbon with  $\text{SO}_3\text{H}$  groups prepared by sulfonation of carbon precursors obtained at moderate carbonization temperatures (673–723 K) exhibits much higher catalytic performance for esterification, transesterification, hydration, and hydrolysis than conventional solid acid catalysts.<sup>14–16</sup> The hydrolysis of  $\beta$ -1,4 glucan by this carbon material is described in this section.

$\beta$ -1,4 glucans are linear polysaccharides of glucose linked by  $\beta$ -1,4 glycosidic bonds, and the hydrolysis of  $\beta$ -1,4 glucan, including cellulose, is an attractive reaction that would allow the use of grasses, and agricultural and wood wastes as a resource for glucose production.<sup>55</sup> Starch (amylose and amylopectin), which consists of polysaccharides of glucose linked by  $\alpha$ -1,4 and  $\alpha$ -1,6 glycosidic linkages ( $\alpha$ -glucan), can be readily decomposed into glucose by amylase and mineral acid catalysts, and large-scale glucose production is possible by such an approach.<sup>55,56</sup> The hydrolysis of cellulose and water-soluble  $\beta$ -1,4 glucans as hydrolysis products of cellulose, however, is more difficult than that of  $\alpha$ -glucan, although the details of the hydrolysis reaction remain to be clarified.<sup>55,57</sup> Naidoo et al. reported that the  $\alpha$ -1,4 and  $\alpha$ -1,6 glycosidic linkages in  $\alpha$ -glucan are flexible in the presence of water, which weakens the intramolecular hydrogen bonds across the glycosidic linkage.<sup>58–60</sup> The  $\alpha$ -1,4 and  $\alpha$ -1,6 glycosidic linkages in  $\alpha$ -glucan are therefore more readily hydrolyzed by a catalyst in the presence of water. Conversely, in

symmetric  $\beta$ -1,4 glucan, the intramolecular hydrogen bonds between the oxygen atoms in glycopyranose rings and the hydroxyl groups across the  $\beta$ -1,4 linkages are the main contributor among all intra- and intermolecular hydrogen bonds to the firm structure of  $\beta$ -1,4 glucan.<sup>61</sup> The intramolecular hydrogen bonds in symmetric  $\beta$ -1,4 glucan (as with cellulose) thus cause even short-chain water-soluble  $\beta$ -1,4 glucan molecules to form tight aggregates in water,<sup>62</sup> protecting the  $\beta$ -1,4 glycosidic bonds in the aggregate from catalytic hydrolysis. This is an obstacle to both acid-catalyzed saccharification and enzymatic hydrolysis of cellulosic biomass. The former requires strong acid catalysts such as  $\text{H}_2\text{SO}_4$ , a homogeneous acid catalyst with a large environmental impact, to decompose hydrogen bonds and  $\beta$ -1,4 glycosidic bonds. Meanwhile, the latter reaction requires a large amount of enzymes to achieve a sufficient saccharide concentration. Any solid acids that have high catalytic performance for the hydrolysis of  $\beta$ -1,4 glucan would be applicable to efficient cellulosic biomass conversion; such solid acids would be used as easily separable and reusable catalysts not only for acid-catalyzed cellulose hydrolysis, but also for the optimization of other industrial reactions. While cellulase can efficiently hydrolyze cellulosic biomass, it does not accommodate an increase in the monosaccharide concentration in an aqueous solution due to biological reasons. Enzymatic saccharification of cellulosic biomass therefore requires a large amount of cellulase to produce a concentrated saccharide solution, which results in increased costs. The hydrolysis of cellulose into short-chain water-soluble  $\beta$ -1,4 glucans, followed by hydrolysis into monosaccharides by solid acid catalysts could be used to produce a concentrated monosaccharide solution, decreasing the amount of used cellulase.

Figure 7 shows the results for the hydrolysis of cellohexaose over various catalysts (363 K). The black bar indicates the total

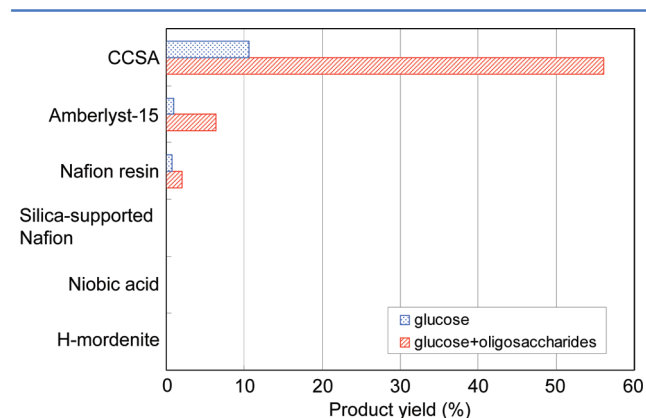


**Figure 7.** Yields of hydrolysis products in hydrolysis of cellohexaose by various solid acid catalysts at 363 K for 1 h (catalyst, 0.30 g; cellohexaose, 5.25 mg; water, 0.70 g).

amounts of water-soluble saccharides produced by hydrolysis (glucose, cellobiose, cellotriose, cellotetraose, cellopentaose). CCSA (673 K) has the highest catalytic performance for the reaction among the solid acids tested. The TOF of  $\text{SO}_3\text{H}$  groups in CCSA is comparable to that of  $\text{H}_2\text{SO}_4$ .<sup>45</sup> The solid acid Amberlyst-15 ( $4.8 \text{ mmol g}^{-1}$ ) has a larger amount of  $\text{SO}_3\text{H}$  groups than CCSA ( $1.8 \text{ mmol g}^{-1}$ ), and Nafion and silica-supported Nafion have stronger acidity ( $H_0 = -11$  to  $-13$ ) than CCSA ( $H_0 = -8$  to  $-11$ ); however, the catalytic activity of CCSA is much higher than these solid acids. This indicates that

the high catalytic performance of CCSA cannot be explained by either the acid amount or the acid strength. One possible explanation for the enhanced hydrolytic performance of this carbon material is the ability of the material to adsorb  $\beta$ -1,4 glucan. The adsorption of  $\beta$ -1,4 glucan to each solid acid catalyst is shown in Figure 8, in terms of the reduction of

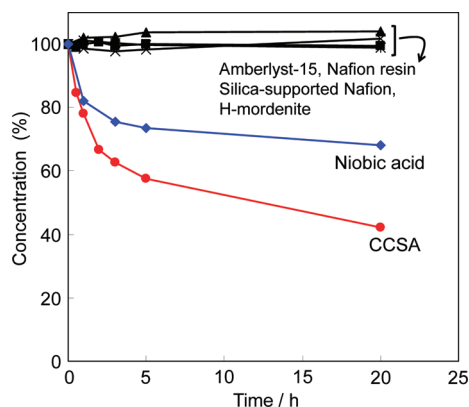


**Figure 8.** Concentrations of celohexaose in celohexaose solutions in the presence of various solid acids at room temperature (298 K).

celohexaose concentrations in the celohexaose solution. In the experiment, 0.1 g of the solid acid was added to 2 cm<sup>3</sup> of each aqueous cellobiose and celohexaose solution (1.5 mmol dm<sup>-3</sup>), and the mixtures were stirred at room temperature (298 K). The results for Amberlite-IRC76, a polystyrene-based cation-exchangeable resin bearing COOH (ca. 4.0 mmol g<sup>-1</sup>), are also shown. The acid strength of Amberlite-IRC76 is insufficient to hydrolyze  $\beta$ -1,4 glucan, and none of the tested catalysts hydrolyzed celohexaose under these conditions. Neither of the water-soluble  $\beta$ -1,4 glucans were adsorbed to H-mordenite or conventional SO<sub>3</sub>H-bearing polymer-based solid acids such as Amberlyst-15, Nafion NR50, and silica-supported Nafion, even after 20 h of stirring. However,  $\beta$ -1,4 glucan was successfully adsorbed to the carbon material and niobic acid. This suggests

that strong Brønsted acid sites on the substrate for  $\beta$ -1,4 glucan to adsorb to will be more efficient in decomposing hydrogen bonds and hydrolyzing  $\beta$ -1,4 glycosidic bonds of  $\beta$ -1,4 glucan than those of nonadsorbing substrates. Thus, hydrolytic activity comparable to that of a homogeneous acid with much higher mobility (i.e., liquid catalyst) can be achieved. The ability of the carbon material to adsorb  $\beta$ -1,4 glucan is due to the presence of hydrophilic functional groups. SO<sub>3</sub>H is not an adsorption site, as demonstrated by the inability of SO<sub>3</sub>H-bearing polymer-based solid acids to adsorb  $\beta$ -1,4 glucan. The results of Figure 8 show that celohexaose adsorbs to COOH groups bonded to polystyrene-based resin (Amberlite-IRC76), although at a rate much lower than that for the carbon material despite the higher density of COOH groups in the resin (ca. 4.0 mmol g<sup>-1</sup> vs ca. 0.4 mmol g<sup>-1</sup>). COOH groups are therefore not the dominant site responsible for the adsorption of  $\beta$ -1,4-glucan to the carbon material. In cellulose, strong intermolecular hydrogen bonds between neutral OH groups in long chain  $\beta$ -1,4-glucans aggregate them. As a result, the ability to adsorb  $\beta$ -1,4 glucan can be attributable to hydrogen bonds by a large amount of phenolic OH groups (2 mmol g<sup>-1</sup>) bonded to the carbon sheets.<sup>16,45</sup>

The strong adsorptive capacity of niobic acid, which possesses a high density of neutral or weakly acidic OH groups, suggests that OH groups are favorable sites for  $\beta$ -1,4 glucan adsorption on both niobic acid and the carbon material. Although niobic acid is capable of adsorbing  $\beta$ -1,4 glucan, this inorganic Brønsted solid acid does not hydrolyze  $\beta$ -1,4 glucan efficiently. In niobic acid with a high density of OH groups, most OH groups are neutral or only weakly acidic, and the density of strongly acidic OH ( $H_0 = -5.6$ ) groups is only 0.4 mmol g<sup>-1</sup>.<sup>63</sup> The acidic OH groups in niobic acid are thus unable to hydrolyze  $\beta$ -1,4 glycosidic bonds, particularly in the presence of water, which substantially reduce the acid catalytic activity of acidic OH groups bonded to a metal oxide.

It should be noted that the carbon material is available for the hydrolysis of  $\beta$ -1,4 glucan without decreasing the activity over a long period. The results for the hydrolysis of cellobiose using a fixed-bed reactor with CCSA are shown in Figure 9; no

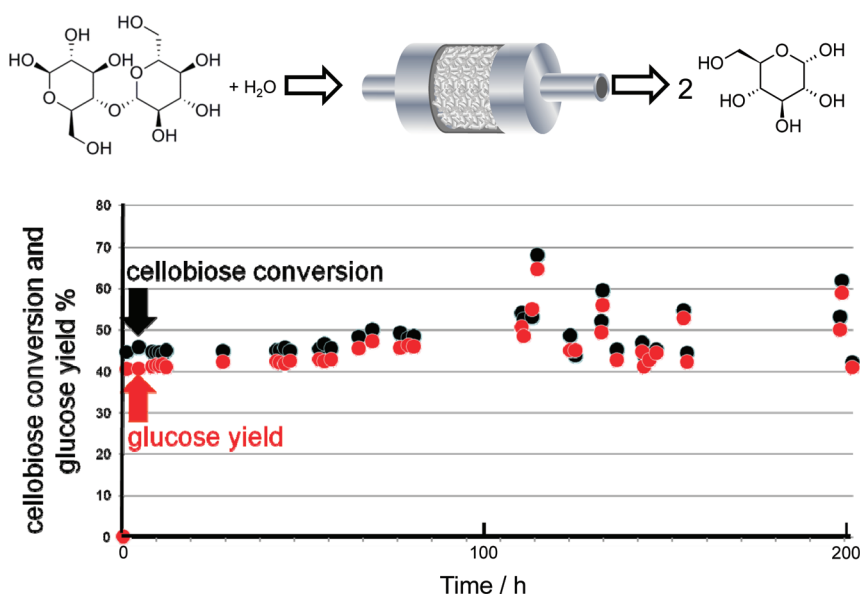


**Figure 9.** Hydrolysis of cellobiose by a fixed-bed reactor with CCSA. Reaction temperature: 373 K, reactor vol.: 11 mL, catalyst: 5.3 g 0.5 wt % cellobiose aqueous solution, 0.1 mL min<sup>-1</sup>.

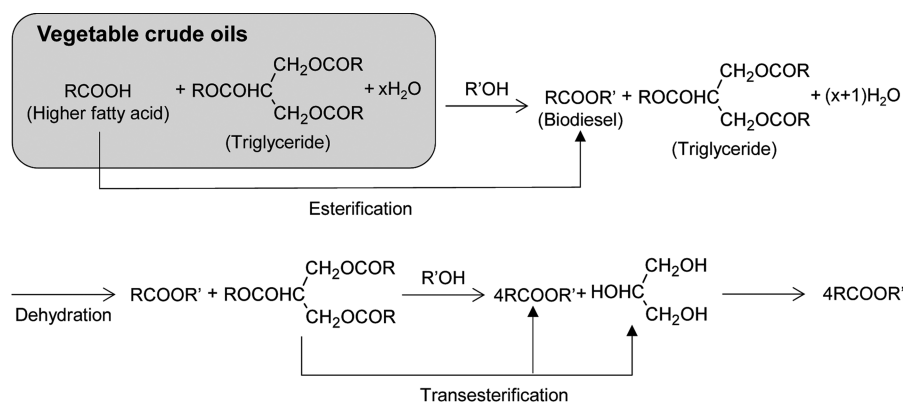


**Figure 10.** Biodiesel production from crude vegetable oils.

decrease in activity was observed, even after 200 h. In addition, no significant difference was observed between cellobiose conversion and glucose yield, which indicates that glucose is not further decomposed into byproduct such as 5-hydroxymethylfurfural, formic acid, and organic acids. This confirms that the carbon material cannot adsorb monosaccharide, which facilitates the efficient hydrolysis without side reactions.<sup>16,45</sup>

Thus, amorphous carbon bearing  $\text{SO}_3\text{H}$ ,  $\text{COOH}$ , and  $\text{OH}$  groups can efficiently hydrolyze not only water-soluble  $\beta$ -1,4 glucan, but also water-insoluble  $\beta$ -1,4 glucan (cellulose) using  $\text{OH}$  groups bonded to carbon sheets for the adsorption of  $\beta$ -1,4 glucan.<sup>16,32</sup> In addition to determining the mode of catalysis based on the structure, the carbon material was also confirmed to have sufficient stability for practical use.

**5.2. Biodiesel Production.** Recently, advances in production technology and changes in the political climate have increased the availability and awareness of biodiesel, an alternative to petroleum-derived diesel fuel with much lower net-sum  $\text{CO}_2$  emissions, due to the absorption of  $\text{CO}_2$  by plants used to produce the fuel. Biodiesel is, in a broad sense, composed of higher fatty acid derivatives, such as fatty acid esters made from triglycerides (esters of higher fatty acids and glycerol) or higher fatty acids in plant materials or animal fat. Crude vegetable oils obtained by compressing plant seeds or fruits, such as soybeans, rapeseed, and palm fruit, are starting materials for large-scale biodiesel production. These crude vegetable oils consist of considerably free, higher fatty acids and water, in addition to triglycerides. It is therefore difficult for any base catalyst to produce biodiesel from crude vegetable oils by base-catalyzed transesterification of triglycerides, because water in the starting materials largely decreases base catalysis, and neutralization of basic active sites in the catalysts by higher fatty acids prevents biodiesel production by transesterification. One process for biodiesel production from crude vegetable oil is schematically shown in Figure 10, which illustrates biodiesel production by the esterification of higher fatty acids and the transesterification of triglycerides. The most popular method is acid-catalyzed esterification, followed by base-catalyzed transesterification. In this process, the use of homogeneous or soluble acid and base catalysts, as in conventional biodiesel production, results in a large environmental load. Although homogeneous acid catalysts such as  $\text{H}_2\text{SO}_4$  exhibit high catalytic performance for the esterification of higher fatty acids, they require special processing in the form of neutralization, in addition to costly and inefficient catalyst separation. The use of soluble base catalysts such as  $\text{KOH}$  for

transesterification of triglycerides in the product obtained by esterification also leads to large energy consumption.

A heterogeneous catalyst that functions as a stable and efficient catalyst for both reactions would be applicable to the environmentally benign production of biodiesel from crude vegetable oils. Solid acid catalysts are promising candidates for this purpose, because acids can catalyze both esterification and transesterification. While the transesterification of triglycerides by acid catalysts usually requires high reaction temperatures of more than ca. 423 K,<sup>64</sup> amorphous carbon bearing  $\text{SO}_3\text{H}$ ,  $\text{COOH}$ , and  $\text{OH}$  groups can efficiently catalyze both reactions under moderate conditions.<sup>13,19,24,26,31,36,39,41,65–67</sup>

Table 3 shows the results of a carbon catalyst reuse experiment for the esterification of oleic acid and methanol at

**Table 3.** Esterification of Oleic Acid in the Presence of  $\text{SO}_3\text{H}$ -Bearing Carbon Material<sup>a</sup>

catalyst reuse	yield of methyl oleate (%)	
	1 h	4 h
fresh	62.0	99.9
1	60.3	99.8
2	65.3	99.6
3	64.2	99.6

<sup>a</sup>Reagents and condition: oleic acid 1.78 g, methanol 5.21 g, catalyst 0.307 g, reaction temperature 368 K, reaction time 1 and 4 h. The recovered catalyst was reused after washing with water and dry at 403 K.

368 K. The methyl oleate yield reaches ca. 90% within 2 h in the presence of the carbon material (CCSA-637). The carbon material exhibits much higher catalytic performance for the reaction than other conventional solid Brønsted acid catalysts tested, such as niobic acid ( $\text{Nb}_2\text{O}_5 \cdot n\text{H}_2\text{O}$ ), Amberlyst-15 (sulfonated polystyrene), and Nafion NRS0 (perfluorosulfonated ionomer),<sup>68</sup> and is 70–80% that of sulfuric acid under the same reaction conditions. After reacting for 4 h, the carbon catalyst was readily precipitated in the reaction vessel, and the precipitated catalyst was repeatedly reused for subsequent reactions after washing with water and drying at 403 K. No decrease in activity was observed even after 10 reuses.

The carbon material also shows high catalytic performance for the transesterification of triolein, as summarized in Tables 4 and 5. While SAC-13, silica-supported Nafion, has a much higher turnover number (TON) for the transesterification than Amberlyst-15 and Nafion NRS0, Amberlyst-15 shows the largest methyl oleate yield due to a high density of  $\text{SO}_3\text{H}$

**Table 4. Transesterification of Triolein by Solid Acids (353 K)**

catalyst	SO <sub>3</sub> H density/mmol g <sup>-1</sup>	yield of methyl oleate (%)	TON
carbon material	1.8	24.1	30.0
Amberlyst-15	4.9	5.0	1.6
Nafion NRS0	0.9	1.5	2.5
Nafion SAC-13	0.1	1.1	14.0

<sup>a</sup>Reagents and condition: catalyst 0.2 g, triolein 0.01 mol, methanol 0.3 mol, reaction temperature 353 K, reaction time 6 h.

**Table 5. Transesterification of Triolein in the Presence of SO<sub>3</sub>H-Bearing Carbon Material (403 K)<sup>a</sup>**

catalyst reuse	yield of methyl oleate (%)	
	2 h	5 h
fresh	50.8	98.1
1	52.0	99.0
2	48.0	94.3
3	50.0	95.5
4	50.3	99.2
5	52.3	96.0

<sup>a</sup>Reagents and condition: triolein 1.7 g, methanol 3.8 g, catalyst 0.40 g, water 0.02 g, reaction temperature 403 K, reaction time 2 and 5 h, pressure 700 kPa. The recovered catalyst was reused after washing with water and dry at 403 K.

groups among the tested conventional solid acids, as shown in Table 4. The carbon material exhibits a much higher methyl oleate yield and TON than the conventional solid acids tested. Table 5 shows the results of a carbon catalyst reuse experiment for the transesterification of triolein and methanol at 403 K under optimal reaction conditions; the material also acts as a stable catalyst for transesterification. These results suggest that the biodiesel production process, shown in Figure 10, could be achieved using only the carbon material as a catalyst.

## 6. OUTLOOK

Amorphous carbon with SO<sub>3</sub>H groups acts as an active, stable, and reusable heterogeneous Brønsted acid catalyst. This can be attributed to the specific carbon network of functional groups bonded to carbon sheets. The carbon material has been produced from waste wood in a middle scale plant and several industrial processes have been tested for a practical application of the catalyst. However, the material is far from being "a replacement catalyst" for homogeneous Brønsted acids from the viewpoint of catalytic performance and processing. Further improvement is required before homogeneous acids can be replaced with amorphous carbon bearing SO<sub>3</sub>H groups.

## AUTHOR INFORMATION

### Corresponding Author

\*Telephone number: +81-45-924-5311. Fax number: +81-45-924-5381. E-mail address: mhara@mssl.titech.ac.jp.

### Notes

The authors declare no competing financial interest.

## ACKNOWLEDGMENTS

This work was supported by the Core Research for Evolutional Science and Technology (CREST, JY230195) program of the Japan Science and Technology (JST) Corporation.

## REFERENCES

- Anastas, P. T.; Kirchoff, M. M. *Acc. Chem. Res.* **2002**, *35*, 686–694.
- DeSimone, J. M. *Science* **2002**, *297*, 799–781.
- Harton, B. *Nature* **1999**, *400*, 797–799.
- Anastas, P. T.; Zimmermann, J. B. *Environ. Sci. Technol.* **2003**, *37*, 94A–101A.
- Clark, J. H. *Acc. Chem. Res.* **2002**, *35*, 791–797.
- Misono, M. *Comp. R. Acad. Sci., Serie II: Chim.* **2000**, *3*, 471–475.
- Okuhara, T. *Chem. Rev.* **2002**, *102*, 3641–3666.
- Smith, K.; El-Hiti, G. A.; Gamal, A.; Jayne, A. J.; Butters, K. *Org. Biomolec. Chem.* **2003**, *1*, 1560–1564.
- Olah, G. A.; Iyer, P. S.; Prakash, G. K. S. *Synthesis* **1986**, *7*, 513–531.
- Inagaki, S.; Guan, S.; Ohsuna, T.; Terasaki, O. *Nature* **2002**, *416*, 304–307.
- Wilson, K.; Lee, A. F.; Macquarie, D. J.; Clark, J. H. *Appl. Catal., A: Gen.* **2002**, *228*, 27–133.
- Cano-Serrano, E.; Campos-Martin, J. M.; Fierro, J. L. G. *Chem. Commun.* **2003**, *247*, 246–247.
- Toda, M.; Takagaki, A.; Okamura, M.; Kondo, J. N.; Hayashi, S.; Domen, K.; Hara, M. *Nature* **2005**, *438*, 178–178.
- Okamura, M.; Takagaki, A.; Toda, M.; Kondo, J. N.; Tatsumi, T.; Domen, K.; Hara, M.; Hayashi, S. *Chem. Mater.* **2006**, *18*, 3039–3045.
- Hara, M.; Yoshida, T.; Takagaki, A.; Takata, T.; Kondo, J. N.; Domen, K.; Hayashi, S. *Angew. Chem., Int. Ed.* **2004**, *43*, 2955–2958.
- Suganuma, S.; Nakajima, K.; Kitano, M.; Yamaguchi, D.; Kato, H.; Hayashi, S.; Hara, M. *J. Am. Chem. Soc.* **2009**, *131*, 12787–12793.
- Nakajima, K.; Okamura, M.; Kondo, J. N.; Tatsumi, T.; Domen, K.; Hayashi, S.; Hara, M. *Chem. Mater.* **2009**, *21*, 186–193.
- Kitano, M.; Yamaguchi, D.; Suganuma, S.; Nakajima, K.; Kato, H.; Hayashi, S.; Hara, M. *Catal. Lett.* **2009**, *131*, 242–249.
- Suganuma, S.; Nakajima, K.; Kitano, M.; Yamaguchi, D.; Kato, H.; Hayashi, S.; Hara, M. *Solid State Sci.* **2010**, *12*, 1029–1034.
- Suganuma, S.; Nakajima, K.; Kitano, M.; Kato, H.; Tamura, A.; Kondo, H.; Yanagawa, S.; Hayashi, S.; Hara, M. *Microporous Mesoporous Mater.* **2011**, *143*, 443–450.
- Fukuhara, K.; Nakajima, K.; Kitano, M.; Kato, H.; Hayashi, S.; Hara, M. *ChemSusChem* **2011**, *4*, 778–784.
- Budarin, V.; Clark, J. H.; Hardy, J. J. E.; Luque, R.; Milkowski, K.; Tavener, S. J.; Wilson, A. J. *Angew. Chem., Int. Ed.* **2006**, *45*, 3782–3786.
- Budarin, V.; Clark, J. H.; Hardy, J. J. E.; Luque, R.; Milkowski, K.; Tavener, S. J.; Wilson, A. J. *Angew. Chem., Int. Ed.* **2006**, *45*, 3782–3786.
- Moa, X.; López, D. E.; Suwannakarn, K.; Liu, Y.; Lotero, E.; Goodwin, J. G., Jr.; Lu, C. *J. Catal.* **2008**, *254*, 332–338.
- Wang, X.; Liu, R.; Waje, M. M.; Chen, Z.; Yan, Y.; Bozhilov, K. N.; Feng, P. *Chem. Mater.* **2007**, *19*, 2395–2397.
- Zong, M.-H.; Duan, Z.-Q.; Lou, W.-Y.; Smith, T. J.; Wu, H. *Green Chem.* **2007**, *9*, 434–437.
- Xing, R.; Liu, Y.; Wang, Y.; Chen, L.; Wu, H.; Jiang, Y.; He, M.; Wu, P. *Microporous Mesoporous Mater.* **2007**, *105*, 41–48.
- Shaabani, A.; Rahmati, A.; Badri, Z. *Catal. Commun.* **2008**, *9*, 13–16.
- Shokrolahi, A.; Zali, A.; Pouretedal, H. R.; Mahdavi, M. *Catal. Commun.* **2008**, *9*, 859–863.
- Clark, J. H.; Budarin, V.; Dugmore, T.; Luque, R.; Macquarrie, D. J.; Strelko, V. *Catal. Commun.* **2008**, *9*, 1709–1714.
- Mo, X.; Lotero, E.; Lu, C.; Liu, Y.; Goodwin, J. G. *Catal. Lett.* **2008**, *123*, 1–6.
- Onda, A.; Ochi, T.; Yanagisawa, K. *Green Chem.* **2008**, *10*, 1033–1037.
- Zhang, B.; Ren, J.; Liu, X.; Guo, Y.; Guo, Y.; Lu, G.; Wang, Y. *Catal. Commun.* **2010**, *11*, 629–632.
- Pang, J.; Wang, A.; Zheng, M.; Zhang, T. *Chem. Commun.* **2010**, *46*, 6935–6937.



- (35) Van de Vyver, S.; Peng, L.; Geboers, J.; Schepers, H.; de Clippel, F.; Gommaes, C. J.; Goderis, B.; Jacobs, P. A.; Sels, B. F. *Green Chem.* **2010**, *12*, 1560–1563.
- (36) Macia-Agullo, J. A.; Sevilla, M.; Diez, M. A.; Fuertes, A. B. *ChemSusChem* **2010**, *3*, 1352–1354.
- (37) Lin, P.; Li, B.; Li, J.; Wang, H.; Bian, X.; Wang, X. *Catal. Lett.* **2011**, *141*, 459–466.
- (38) Gorityala, B. K.; Ma, J.; Pasunooti, K. K.; Cai, S.; Liu, X.-W. *Green Chem.* **2011**, *13*, 573–577.
- (39) Geng, L.; Wang, Y.; Yu, G.; Zhu, Y. *Catal. Commun.* **2011**, *13*, 26–30.
- (40) Gupta, P.; Paul, S. *Green Chem.* **2011**, *13*, 2365–2372.
- (41) Rao, B. V. S. K.; Chandra Mouli, K.; Rambabu, N.; Dalai, A. K.; Prasad, R. B. N. *Catal. Commun.* **2011**, *14*, 20–26.
- (42) Wang, J.; Xu, W.; Ren, J.; Liu, X.; Lu, G.; Wang, Y. *Green Chem.* **2011**, *13*, 2678–2681.
- (43) Tsubouchi, N.; Xu, C.; Ohtsuka, Y. *Energy Fuels* **2003**, *17*, 1119–1125.
- (44) Ferrari, A. *Phys. Rev. B* **2000**, *61*, 14095–14107.
- (45) Kitano, M.; Yamaguchi, D.; Sugauma, S.; Nakajima, K.; Kato, H.; Hayashi, S.; Hara, M. *Langmuir* **2009**, *25*, 5068–5075.
- (46) Zettlemoyer, A. C.; Young, G. D.; Chessick, J. J.; Healey, F. H. *J. Phys. Chem.* **1953**, *57*, 649–652.
- (47) Dacey, J. R.; Clunie, J. C.; Thomas, D. G. *Trans. Faraday Soc.* **1958**, *54*, 250–256.
- (48) Huo, H.; Peng, L.; Grey, C. P. *J. Phys. Chem. C* **2009**, *113*, 8211–8219.
- (49) Batamack, P.; Doremieux-Morin, C.; Fraissard, J.; Freude, D. *J. Phys. Chem.* **1991**, *95*, 3790–3796.
- (50) Tabony, J. *Prog. Nucl. Magn. Reson. Spectrosc.* **1980**, *14*, 1–26.
- (51) Tabony, J.; Bomchil, G.; Harris, N. M.; Leslie, M.; White, J. W.; Gamlen, P. H.; Thomas, R. K.; Trewern, T. D. *J. Chem. Soc. Faraday Trans.* **1979**, *75*, 1570–1586.
- (52) Tabony, J.; White, J. W.; Delachaume, J. C.; Coulon, M. *Surf. Sci. Lett.* **1980**, *95*, 282–288.
- (53) Myers, K. J. *Molecular Magnetism and Magnetic Resonance Spectroscopy*; Prentice Hall: Upper Saddle River, NJ, 1973.
- (54) Oh, W.-C.; Bae, N.-K.; Cho, Y.-J.; Ko, Y.-S. *Carbon* **1995**, *33*, 323–327.
- (55) Chheda, J. N.; Huber, G. W.; Dumesic, J. A. *Angew. Chem., Int. Ed.* **2007**, *46*, 7164–7183.
- (56) Nagamori, M.; Funazukuri, T. *J. Chem. Technol. Biotechnol.* **2004**, *79*, 229–233.
- (57) Klemm, D.; Heublein, B.; Fink, H. P.; Bohn, A. *Angew. Chem., Int. Ed.* **2005**, *44*, 3358–3393.
- (58) Naidoo, K. J.; Brady, J. W. *J. Am. Chem. Soc.* **1999**, *121*, 2244–2252.
- (59) Best, R. B.; Jackson, G. E.; Naidoo, K. J. *J. Phys. Chem. B* **2001**, *105*, 4742–4751.
- (60) Chen, J. Y.; Naidoo, K. J. *J. Phys. Chem. B* **2003**, *107*, 9558–9566.
- (61) Tashiro, K.; Kobayashi, M. *Polymer* **1991**, *32*, 1516–1526.
- (62) Klemm, D.; Philipp, B.; Heinze, T.; Heinze, U.; Wagenknecht, W. *Comprehensive Cellulose Chemistry*; Wiley-VCH: Weinheim, Germany, 1998.
- (63) Siril, P. F.; Cross, H. E.; Brown, D. R. *J. Mol. Catal. A: Chem.* **2008**, *279*, 63–68.
- (64) Serio, M. D.; Tesser, R.; Pengmei, L.; Santacesaria, E. *Energy Fuels* **2008**, *22*, 207–217.
- (65) Takagaki, A.; Toda, M.; Okamura, M.; Kondo, J. N.; Hayashi, S.; Domen, K.; Hara, M. *Catal. Today* **2006**, *116*, 157–161.
- (66) Hara, M. *ChemSusChem* **2009**, *2*, 129–135.
- (67) Nakajima, K.; Hara, M. *J. Am. Ceram. Soc.* **2008**, *90*, 3725–3734.
- (68) López, D. E.; Goodwin, J. G.; Bruce, D. A. *J. Catal.* **2009**, *245*, 381–391.